KfK 5354
Mai 1994

Electrochemical Corrosion Studies on a Selected Carbon Steel for Application in Nuclear Waste Disposal Containers: Influence of Chemical Species in Brines on Corrosion

A. M. Farvaque-Béra, E. Smailos
Institut für Nukleare Entsorgungstechnik

Kernforschungszentrum Karlsruhe

Kernforschungszentrum Karlsruhe
Institut für Nukleare Entsorgungstechnik

KfK 5354

Electrochemical Corrosion Studies on a Selected Carbon Steel for Application in Nuclear Waste Disposal Containers: Influence of Chemical Species in Brines on Corrosion

A.M. Farvaque-Béra, E. Smailos

Kernforschungszentrum Karlsruhe GmbH, Karlsruhe

Kernforschungszentrum Karlsruhe GmbH
Postfach 3640, 76021 Karlsruhe

ISSN 0303-4003

Summary

In previous corrosion studies, carbon steels were identified as promising materials for the manufacture of long-lived high-level waste containers that could act as an engineered barrier in a rock-salt repository. In this paper, the influence of chemical species, potentially present in salt brines, on the electrochemical corrosion behavior of the preselected fine-grained steel TStE 355 was studied. The steel was examined at 90°C in a disposal relevant NaCl-rich brine containing various species (Br^-, I^-, Cu^{2+}, Mn^{2+}, S^{2-}, $B(OH)_4^-$ and Fe^{3+}) at concentrations between 10^{-5} M/l and 10^{-1} M/l.

The polarization curves indicate that with all potentials applied, the steel exhibits active corrosion. No susceptibility to local corrosion was observed. Bromide (7×10^{-3} M/l - 7×10^{-2} M/l) and iodide (10^{-4} M/l - 10^{-3} M/l) additions to the brine at pH = 7 do not significantly influence the polarization behavior of the steel. In sulfide-containing brines (6×10^{-4} M/l - 6×10^{-3} M/l) at pH = 7, a higher free corrosion potential of -1040 mV was measured compared to the value in the sulfide-free brine (-1155 mV). This increase is attributed to the formation of a layer consisting of FeS and FeS_2 on the specimen surface. However, this does not cause an increase in the spontaneous (initial) corrosion rate. When $MnCl_2 \times 4H_2O$ (9×10^{-4} M/l - 9×10^{-3} M/l) was added to the brine at pH = 7, a change in the cathodic polarization process from charge-transfer to diffusion polarization was observed which is attributed to the formation of the $Mn(OH)_2$ detected on the specimen surface. This change is linked with an increase in the initial corrosion rate from 0.096 mm/a in the Mn^{2+}-free brine to 0.24 mm/a in the Mn^{2+}-containing brine. Additions of $CuCl_2 \times 2H_2O$, H_3BO_3 and $FeCl_3 \times 6H_2O$ to the brine at concentrations between 10^{-5} and 10^{-1} M/l cause at pH = 7 an increase in the initial corrosion rate by a factor 3-5. The increase in the corrosion rate is higher with decreasing pH of the brine.

Long-term immersion experiments are in progress to examine whether species such as Cu^{2+}, $B(OH)_4^-$ and Fe^{3+} can also influence the final corrosion rate of the steel which is of decisive importance for long-term predictions of the container lifetime. Furthermore, the synergistic effects of species present in the bulk brine environments will be investigated.

Elektrochemische Korrosionsuntersuchungen an Kohlenstoffstahl als Behälterwerkstoff zur Endlagerung radioaktiver Abfälle: Einfluß von chemischen Spezies in Salzlösungen auf die Korrosion.

Zusammenfassung

Bisherige Korrosionsuntersuchungen ergaben, daß Kohlenstoffstähle aussichtsreiche Materialien für langzeitbeständige Behälter zur Endlagerung von hochradioaktiven Abfällen in Steinsalzformationen sind. In dieser Arbeit wurde mittels potentiodynamischer Polarisationsmessungen der Einfluß möglicher chemischer Spezies in einer endlagerrelevanten Salzlösung auf das Korrosionsverhalten des ausgewählten Feinkornbaustahls TStE 355 untersucht. Der Stahl wurde bei 90°C in einer NaCl-reichen Lösung untersucht, die unterschiedliche Spezies (Br^-, I^-, Cu^{2+}, Mn^{2+}, S^{2-}, $B(OH)_4^-$ und Fe^{3+}) in Konzentrationen zwischen 10^{-5} und 10^{-1} M/l enthielt.

Die Polarisationskurven zeigen, daß bei allen untersuchten Potentialen der Stahl aktiv korrodiert. Lochkorrosion trat nicht auf. Bromidionen (7×10^{-3} M/l - 7×10^{-2} M/l) und Iodidionen (10^{-4} M/l - 10^{-3} M/l) in der Lösung zeigen bei pH = 7 keinen signifikanten Einfluß auf das Polarisationsverhalten des Stahls. In sulfidhaltigen Lösungen (6×10^{-4} M/l - 6×10^{-3} M/l) bei pH = 7 wurden höhere Freie Korrosionspotentiale von -1045 bis -1040 mV im Vergleich zu der sulfidfreien Lösung (-1155 mV) gemessen. Dies wird auf die Bildung einer aus FeS und FeS_2 bestehenden Schicht auf der Probenoberfläche zurückgeführt. Trotz dieses Effektes wurde kein Anstieg der spontanen Korrosionsrate (Anfangskorrosionsrate) beobachtet. Bei Zusatz von Manganionen in die Salzlösung bei pH = 7 wurde eine Änderung des kathodischen Polarisationsprozesses beobachtet, was auf die nachgewiesene Bildung einer $Mn(OH)_2$-Schicht auf der Probenoberfläche zurückgeführt wird. Diese Änderung ist mit einem Anstieg der Anfangskorrosionsrate etwa um den Faktor 2 verbunden. Zusätze von $CuCl_2 \times 6H_2O$, H_3BO_3 und $FeCl_3 \times 6H_2O$ in der NaCl-reichen Lösung bewirken bei pH = 7 einen Anstieg der Anfangskorrosionsrate um den Faktor 3-5. Mit abnehmendem pH der Lösung nimmt die Korrosionsrate des Stahls weiter zu.

Inwieweit Cu^{2+}, $B(OH)_4^-$ und Fe^{3+} in Salzlösungen einen Einfluß auch auf die Endkorrosionsrate des Stahls haben, die für die Auslegung der Behälterwandstärke entscheidend ist, soll durch Langzeit-Immersionsexperimente geklärt werden. Darüberhinaus soll der synergetische Effekt mehrerer chemischer Spezies in der Lösung auf die Korrosion des Stahls untersucht werden.

Table of content

---

1. Introduction and objectives

According to the German waste disposal concept, the heat-generating nuclear waste such as vitrified high-level waste and spent fuel will be disposed of in repositories located in deep rock-salt formations. The isolation of the radionuclides from the biosphere is to be ensured by a combination of geological and engineered barriers. One element of this multi-barrier concept is the waste packaging. Consequently, studies have been undertaken by KfK within the framework of the European Community research programme to qualify materials for long-lived packagings that could serve as a radionuclide barrier during the elevated-temperature phase in the disposal area which lasts a few hundred years. The main requirement made on the packaging materials is their corrosion resistance in rock salt and salt brines. Salt brines in the disposal area may originate from the thermal migration of brine inclusions in the rock salt and have to be considered in accident scenarios, e.g. brine inflow through an anhydride layer.

In previous corrosion studies on a wide range of materials [e.g. 1, 2, 3, 4], carbon steels were identified as promising materials for the manufacturing of long-lived containers surrounding the Cr-Ni steel waste canisters. Their promising nature is based primarily on the fact that so far only general corrosion has been observed in brine environments so that the long-term corrosion behavior of the steels can be reasonable predicted. Furthermore, the corrosion rates of the actively corroded steels available so far imply acceptable corrosion allowances for thick-walled containers.

To characterize the corrosion behavior of carbon steels in more detail, further electrochemical studies and long-term immersion experiments are being performed in salt brines. An important aspect of the corrosion studies is the investigation of the influence of chemical species present in the bulk brine environments on the corrosion behavior of the steels. According to the literature [5], a large number of salt impurities such as Br^-, Cu^{2+}, $B(OH)_4^-$, S^{2-} etc. are present in brines. In addition, container corrosion will generate Fe^{2+} that may be oxidized to Fe^{3+} by radiolysis of the brines or oxygen ingress into the disposal area. Such species can affect the corrosion behavior of the steels by formation of complexes (e.g. Br^-, I^-) or by causing changes in the redox potential (e.g. Fe^{3+}, S^{2-}, Cu^{2+}). Therefore, potentiodynamic polarization studies were performed in the present work on a preselected carbon steel (fine-grained steel TStE 355) to evaluate the individual influence of some important chemical species (Section 2.1).

2. Experimental

2.1 Test conditions

The chemical composition of the fine-grained structural steel investigated is given in Table 1. The steel specimens were fabricated as disks having a diameter of 10 mm and a thickness of 4 mm. For surface preparation, the specimens were polished with 320, 800 and 1200 grit silicon carbide paper and cleaned with soap and isopropanol.

The corrosion of the steel was studied at 90°C in a disposal relevant NaCl-rich brine (composition see Table 2) using the potentiodynamic polarization method. The selected chemical species Br^-, I^-, Cu^{2+}, $B(OH)_4^-$, S^{2-} and Fe^{3+} were added individually to the brine as sodium salts for anions (except for borate ions which were introduced as boric acid) and as chloride salts for cations. Species concentrations were taken from literature data of rock salt repository analyses reported by Herrmann [5]. Two concentrations were selected for each species: One corresponds to the maximum value indicated in the literature, the other is by one order of magnitude higher or lower. The chemical species and their concentrations used in the experiments are listed in Table 3. After addition of $CuCl_2 \times 2H_2O$, H_3BO_3, $FeCl_3 \times 6H_2O$ and $Na_2S \times 9H_2O$, pH-changes of the brine occurred. The potentiodynamic polarization tests were conducted both with and without pH-correction to the initial value of the brine (pH(25°C) = 7). For the correction of the pH value, 1 m NaOH or 1 m HCl was used.

The experimental set-up consisted of an electrochemical three-compartment cell containing the fine-grained steel specimen as part of the working electrode, a saturated $Hg/Hg_2SO_4/SO_4^{2-}$ reference electrode, a platinium counter electrode, and a potentiostat (P.A.R. model 273) coupled to a computer data acquisition system [3].

2.2 Test procedure

Before the electrochemical measurements started, the salt brine within the cell was deaerated by sparging with a fine stream of argon bubbles for half an hour. Then, the free corrosion potential of the steel in the brine with and without chemical species added at 90°C and pH = 7, was recorded for 30-90 min until it reached a constant value. The free corrosion potential is dependent on the experimental conditions (brine composition, presence of oxidative species, surface state of the specimen) and reflects the nature of corrosion processes which take place at the steel surface (active/passive behavior, layer formation).

Subsequently, potentiodynamic polarization tests were conducted on the steel in the brine with and without additions of chemical species in order to get information on general and local corrosion. For this purpose, the specimens were polarized cathodically from free corrosion potential (E_{corr}) to -250 mV vs. E_{corr} and anodically from free corrosion potential to +1500 mV vs. E_{corr}. The scan rate was 0.2 mV/s. The following polarization parameters were obtained from the polarization curves of potential (E) versus logarithm of the current density (log i):

Free corrosion potential (E_{corr}) and Tafel slopes (b_a, b_c), which are representative of anodic and cathodic corrosion processes, and the corrosion current density (i_{corr}), which permits to calculate the spontaneous (initial) corrosion rate (v_{corr}). All potential values were measured and recorded versus the $Hg/Hg_2SO_4/SO_4^{2-}$ reference electrode (R.E.). Each experiment was repeated at least twice.

After electrochemical testing, the specimens were examined for general and local corrosion by optical and scanning electron microscopy. Analysis of corrosion products was performed by means of the ESCA spectroscopy.

3. Results and discussion

3.1 Free corrosion potential of the fine-grained steel TStE 355 in NaCl-rich brine with and without additions

The time-dependence of the free-corrosion potentials at 90°C measured at pH = 7 in the pure brine and in the brines containing the highest concentration of chemical species, is shown in Fig. 1. From the results obtained, the following statements can be made:

- In all salt brines (except those containing sulfide ions), the free corrosion potentials of the specimens show only low variations of ±20 mV. This indicates that no protective layer develops on the specimens surface. After one hour of immersion into these brines, the free corrosion potentials in all brines reach a constant value of -1155 ±20 mV vs. R.E.
- In the sulfide containing brines (6×10^{-4} M/l and 6×10^{-3} M/l), the free corrosion potentials (Fig. 2) strongly increase with time. After running a maximum of -1010 mV, values of about -1035 mV establish at the end of 90 minutes which are significantly higher than those in the sulfide-free brine (-1155 mV). Furthermore, the maximum value occurs faster for the brine

containing the highest sulfide concentration. This is an indication of the faster formation of a corrosion surface layer (see Section 3.2.6). However, the sulfide concentration has no influence on the value of the final free corrosion potential.

3.2 Polarization behavior of the fine-grained steel TStE 355 in NaCl-rich brine

3.2.1 Pure brine

Figure 3 shows the potentiodynamic polarization curve in the pure salt brine (standard curve). This curve is typical of the active corrosion of a metal. No passivity and no susceptibility to localized corrosion are observed in the region between the corrosion potential and values up to +900 mV vs. R.E.. The anodic and cathodic branches show charge-transfer polarization (taking-on or giving-off electrons is rate-determining). Consequently, anodic and cathodic Tafel slopes of 43 and 103 mV/dec., respectively, were determined. As cathodic reaction, the reduction of water forming molecular hydrogen, and as anodic reaction the oxidation of iron to Fe^{2+} are considered. The initial corrosion rate in the pure brine determined by the Tafel Plot method yields a value of 0.096 mm/a (Table 4).

3.2.2 Influence of bromide and iodide ions

As halides such as bromides and iodides can form soluble complexes with iron, destroy the passive layer of metals, and cause pitting corrosion [6], the potential influence on the corrosion of the steel in the brine was tested. Polarization curves in Br^- (7×10^{-3} M/l and 7×10^{-2} M/l) and I^- (10^{-4} M/l and 10^{-3} M/l) containing brines are given in Figs. 4 and 5. It is shown that under the experimental conditions additions of Br^- and I^- do not change the polarization behavior of the steel compared to that in the pure brine. Consequently, no significant change of the corrosion parameters and rates were found (Table 4). At the end of the tests, a non-uniform corrosion was observed on the surface of the anodically polarized specimens.

3.2.3 Influence of cupric ions

After addition of 7×10^{-5} and 7×10^{-4} M/l $CuCl_2 \times 2H_2O$ to the salt brine, the pH was found to decrease from 7 to 5.8 and 5.0, respectively. Polarization curves of the steel, measured both in the pure brine and in the Cu^{2+}-containing brines with and without pH-correction, are shown in Figs. 6 and 7.

In the Cu^{2+}-containing brines without correction of pH the values of the free corrosion potential, the cathodic Tafel slope and the corrosion current density are clearly higher than in the pure brine (Table 5). After pH-adjustment to the initial value, the following results were obtained in the Cu^{2+}-containing brines (Table 4):

- The values of the free corrosion potentials are very close to that in the pure brine.
- At high cathodic overpotentials discontinuities occurred in the polarization curves.
- The spontaneous corrosion rates of 0.31-0.43 mm/a are clearly higher than that in the Cu^{2+}-free brine (0.096 mm/a). However, the increase in the corrosion current densities for the brine with pH-correction and thus the corrosion rates are much lower than those without pH-correction.
- As in the pure brine, in both cases with and without pH-correction, no passivity and no susceptibility to localized corrosion were obtained in the Cu^{2+}-containing brines. At the end of the cathodic polarization tests, the steel specimens were covered with a thin red film, which is probably metallic copper according to the reaction $Cu^{2+} + 2e^- \rightarrow Cu$. The reduction of the Cu^{2+}-ions explains the discontinuities in the cathodic polarization curves and the increase in the initial corrosion rate.

3.2.4 Influence of manganese ions

Polarization tests were performed in the NaCl-rich brine with additions of Mn^{2+} ions at concentrations of 9×10^{-4} M/l and 9×10^{-3} M/l. The results obtained in the Mn^{2+}-containing brines are given in Fig. 8 and Table 4.

The results show:

- The steel corrodes in an active manner.
- The free corrosion potentials are only slightly higher than in the Mn^{2+}-free brine.
- The cathodic Tafel slopes increase by a factor of about 2 - 2.7 compared to the pure brine which is an indication of a change in the cathodic polarization process from electron charge-transfer to diffusion polarization.

- The initial corrosion rates increase from 0.096 mm/a in the Mn^{2+}-free brine to 0.22-0.24 mm/a.

In order to be able to explain the change in the cathodic polarization process, ESCA-analyses of adherent corrosion products were conducted on three specimens. For the analyses, specimens were selected, which were examined at the highest Mn^{2+}-concentration of the brine with and without polarization.

- Specimen 1 was maintained at free-corrosion potential (-1146 mV) for 2 hours.
- Specimen 2 was cathodically polarized from free corrosion potential to -1400 mV vs. R.E. at the low scan rate of 0.2 mV/s.
- Specimen 3 was polarized potentiostatically at -1300 mV vs. R.E. (cathodic polarization) for 30 minutes.

The results obtained (Figs. 9-11 and Table 6) show variations among the three specimens concerning

- the ratio of Mn to Fe in the adherent corrosion products,
- the form of the oxygen-multiplet (ratio of oxide to hydroxide) in the ESCA-spectrum,
- the concentration of other ions such as Mg^{2+}, Cl$^-$ and Na$^+$ (constituents of the brine).

The following results were obtained for the single specimens:

Specimen 1: The covering corrosion layer consists mainly of FeOOH, as is evident from the typical form of the O1s multiplet (Fig. 9). This thin layer (nm range) covers the entire surface area of the specimen. In addition to FeOOH, manganese probably as $Mn(OH)_2$ or MnO with the ratio Mn/Fe = 0.20-0.25 was detected. Furthermore, Mg^{2+}, but no Cl$^-$, were detected in the layer. After repeated washing with demineralized water, no significant decrease of the Mg^{2+} content was found. This could be explained by the fact that Mg^{2+} are available in the insoluble form, perhaps as $Mg(OH)_2$ or MgO.

Specimen 2: The covering layer of this specimen consists of nearly the same amounts of Fe and Mn (Table 6). Iron is present mainly as Fe^{3+}, but a small amount of Fe_o was also detected. The presence of Fe_o is attributed to the fact that the layer is extremely thin so that the bulk material itself was measured too. Manganese is probably present as $Mn(OH)_2$, MnO or $MnCl_2$. Anyway, the content of Cl$^-$ is not sufficient to explain the formation of exclusively $MnCl_2$ (Mn/Cl theor.

= 2).The form of the O_{1s}-multiplet (Fig. 10) shows the predominance of the Fe-, Mn- or Mg-hydroxides over the oxides. In addition, brine constituents such as Mg^{2+}, Cl^- and Na^+ were detected.

Specimen 3: Mn^{2+}-products were found to predominate on this specimen (Table 6). As for specimen 2, the iron is present above all as Fe^{3+}, but a small amount of Fe_o was also detected which indicates again that the bulk material was involved in the measurement. The oxide/hydroxide ratio is the smallest observed, compared to the other two specimens. Cl^-, Mg^{2+} and Na^+ ions were found as impurities resulting from the brine. The Cl^--content was twice that for specimen 2, the Na^+-content corresponded to that of specimen 2.

The results of the ESCA-analyses show that in the case of the cathodically polarized specimens higher amounts of Mn^{2+} and OH^- occur, compared to those for the specimens tested at the free corrosion potential. The reason for this is that by cathodic polarization the reduction of water leads to the formation of a large amount of OH^- which can associate with Mn^{2+} and forms $Mn(OH)_2$. Consequently, the larger values of the cathodic Tafel slope b_c are attributed to diffusion effects in the system, i.e. to concentration-polarization effects.

3.2.5 Influence of borate ions

Borate ions can enhance the passivation process of low carbon, steels in aqueous solutions [7] and consequently may increase the susceptibility to localized corrosion. Under this aspect, polarization experiments were performed on the fine-grained steel in the brine containing boric acid at concentrations of 1.4×10^{-2} and 1.4×10^{-1} M/l. The results are summarized in Tables 4 and 5. By addition of boric acid to the brine the pH value decreased from 7 to 5.4 and 4.6, respectively. Polarization tests without pH-correction show for the steel (Fig. 12):

- No tendency to passivity and no susceptibility to localized corrosion.
- Increase in the free corrosion potential from -1155 mV in the pure brine up to -1100 mV in the borate containing brines. This effect is attributed to the decrease of pH.
- High increase in the corrosion current densities and thereby in the corrosion rate.

After adjustment of the pH of the brine to the initial value of 7, the following results were obtained in the borate ion-containing brines compared to the pure brine (Fig. 13):

4. Conclusions

From the electrochemical corrosion studies on the preselected container material fine-grained steel TStE 355 at 90°C, the following conclusions can be drawn:

- In NaCl-rich brine with and without chemical species such as Br^-, I^-, S^{2-}, Mn^{2+}, Cu^{2+}, $B(OH)_4^-$ and Fe^{3+}, the steel is subjected to non-uniform general corrosion. Pitting corrosion in the sense of an active-passive corrosion element was not observed.
- Br^- (7×10^{-3} - 7×10^{-2} M/l), I^- (10^{-4} - 10^{-3} M/l) and S^{2-} (6×10^{-4} - 6×10^{-3} M/l) in the brine do not enhance the initial corrosion rate of the steel beyond the value in the pure brine.
- Mn^{2+} (9×10^{-4} - 9×10^{-3} M/l) in the brine increases the initial corrosion rate by a factor of about 2 compared to the value in the Mn^{2+}-free brine.
- Cu^{2+} (7×10^{-5} - 7×10^{-4} M/l), $B(OH)_4^-$ (1.4×10^{-2} - 1.4×10^{-1} M/l) and Fe^{3+} (3.5×10^{-3} - 3.5×10^{-2} M/l) in the brine accelerate the initial corrosion rate by a factor of about 3-5. The increase in the corrosion rate is higher with decreasing pH of the brine.

In addition to electrochemical studies, immersion experiments are in progress by which it is examined whether species such as Cu^{2+} $B(OH)_4^-$ and Fe^{3+} can influence the long-term corrosion rate of the steel which is important to the thickness of the container wall. Furthermore, the synergistic effects of species present in the bulk brine environments will be investigated.

Acknowledgements

The authors thank Prof. Dr. Jae Il Kim for reviewing this paper, Mrs. G. Pfennig for the ESCA-analyses of corrosion products, and Mrs. B. Bennek-Kammerichs for the metallographic examination of the specimens.

5. References

[1] E. Smailos, W. Schwarzkopf, R. Storch

"Corrosion Studies on Packaging Materials for High-Level Waste Disposal in a Rock-Salt Repository", Proc. of the 12th Scandinavian Corrosion Congress and Eurocorr 92", Espoo, Finland, June 1992, pp. 327-338.

[2] E. Smailos, W. Schwarzkopf, B. Kienzler, R. Köster

"Corrosion of Carbon Steel Containers for Heat-Generating Nuclear Waste in Brine Environments Relevant for a Rock-Salt Repository", Mat. Res. Soc. Symp. Proc., Vol 257, pp. 399-406 (1992).

[3] A.M. Farvaque-Béra, S. Leistikow

"Electrochemical Studies of the Corrosion Behavior of a Low Carbon Steel in Simulated Salt Repository Environments", Proc. of the 12th Scandinavian Corrosion Congress and Eurocorr 92", Espoo, Finland, June 1992, pp. 339-347.

[4] E. Smailos, W. Schwarzkopf, R. Köster, K.H. Grünthaler

"Advanced Corrosion Studies on Selected Packaging Materials for Disposal of HLW Canisters in Rock Salt", Proc. of Waste Management '88", Tucson, Arizona, USA, Vol. 2, pp. 985-994 (1988).

[5] A.G. Herrmann

"Über das Vorkommen einiger Spurenelemente in Salzlösungen aus dem deutschen Zechstein", Kali und Steinsalz, 3, S. 209-220 (1961).

[6] G.H. Wagner

"Pitting Corrosion", in Stainless Steel Europe, p. 45 (October 1992).

[7] P.W. Reimus

"Localized Corrosion of Mild Steel Nuclear Waste Package Containers", PNL/SRP-6662, 2, pp. 8-9 (1987).

[8] M. Fischer, W. Gruner, G. Reinhard

"Zum Einfluß des Borat-Anions auf die elektrochemischen Eigenschaften des Eisens in wäßrigen Lösungen", Corr. Sci., 15, pp. 279-293 (1975).

[9] A.M. Farvaque-Béra, H. von Berg

"Elektrochemische Korrosionsuntersuchungen am Feinkornbaustahl TStE 355 als Werkstoff für Endlagerbehälter: Korrosionsverhalten in sulfidhaltigen Lösungen", KfK 5319 (1994).

[10] G.I. Ogundele, W.E. White

"Some Observations on the Corrosion of Carbon Steel in Sour Gas Environments", Corr. NACE, 42 (7), pp. 398-408 (1986).

Table 1: Chemical composition (wt.%) of the fine-grained steel TStE 355 tested in salt brines

C	Si	Mn	P	S	Fe
0.17	0.44	1.49	0.02	0.04	bal.

Table 2: Chemical composition (wt.%) of the NaCl-rich brine used in the corrosion experiments

NaCl	$MgSO_4$	K_2SO_4	$CaSO_4$	H_2O
25.9	0.16	0.24	0.20	73.5

Table 3: Chemical species and their concentrations examined in the corrosion studies on fine-grained steel in a NaCl-rich brine

Chemical species	Added to the brine as	Concentration (mM/l)	
Br^-	NaBr	7	70
I^-	NaI	0.1	1
Cu^{2+}	$CuCl_2x2H_2O$	0.07	0.7
Mn^{2+}	$MnCl_2x4H_2O$	0.9	9
$B(OH)_4^-$	H_3BO_3	14	140
S^{2-}	Na_2Sx9H_2O	0.6	6
Fe^{3+}	$FeCl_3x6H_2O$	3.5	35

Table 4: Results of the electrochemical corrosion studies on the fine-grained steel TStE 355 in the NaCl-rich brine with and without additions of chemical species (T = 90 °C, pH = 7)

Added chemical species	Concentration (mM/l)	E_{corr} (mV vs R.E.)	b_a (mV/dec)	b_c (mV/dec)	I_{corr} ($\mu A/cm^2$)	U_{corr} (mm/a)
no	-	-1155	43	103	8.3	0.096
Br^-	7	-1167	39	110	5.5	0.064
	70	-1160	39	112	7.0	0.081
I^-	0.1	-1152	41	112	9.8	0.10
	1	-1156	41	123	11.0	0.13
Cu^{2+}	0.07	-1160	46	173	23	0.31
	0.7	-1155	42	156	37	0.43
Mn^{2+}	0.9	-1140	40	201	19	0.22
	9	-1146	44	267	21	0.24
$B(OH)_4^-$	14	-1135	45	134	31	0.36
	140	-1130	50	136	45	0.52
S^{2-}	0.6	-1045	42	420	6.0	0.07
	6	-1040	39	455	10.5	0.12
Fe^{3+}	3.5	-1158	75	116	37	0.43
	35	-1171	60	105	25	0.29

E_{corr} = free corrosion potential
ba, bc = anodic and cathodic Tafel slopes
I_{corr} = corrosion current density
U_{corr} = initial corrosion rate

Table 5: Results of the electrochemical corrosion studies on the fine-grained steel TStE 355 in the NaCl-rich test brine with and without additions of chemical species at 90°C and various pH-values

Added chemical species	Concentration (mM/l)	pH	E_{corr} (mV vs R.E.)	b_a (mV/dec)	b_c (mV/dec)	I_{corr} (μA/cm^2)
no	-	7	-1155	43	103	8.3
Cu^{2+}	0.07	5.8	-1138	42	222	90
	0.07	7	-1160	46	173	23
	0.7	5.0	-1080	40	450	112
	0.7	7	-1155	42	156	37
$B(OH)_4^-$	14	5.4	-1121	54	210	120
	14	7	-1135	45	134	31
	140	4.6	-1100	62	170	440
	140	7	-1130	50	136	45
Fe^{3+}	3.5	2.7	-960	107	205	1400
	3.5	7	-1158	75	116	27
	35	2.4	-937	150	242	4500
	35	7	-1171	60	105	35

Table 6: Results of the ESCA-analyses of adherent corrosion products on TStE 355-specimens after testing in Mn^{2+}-containing NaCl-rich brine (relative concentrations)

Specimen No.	Mn	Fe	Mg	Cl	Na	O^{2-}	OH^-
1	1.0	4-5	1.0	n.d.	traces	7.0	7.2
2	1.0	1.0	0.3	0.3	traces	1.6	2.7
3	1.0	0.2-0.3	0.2	0.6	traces	0.7	2.0

n.d.: not detected

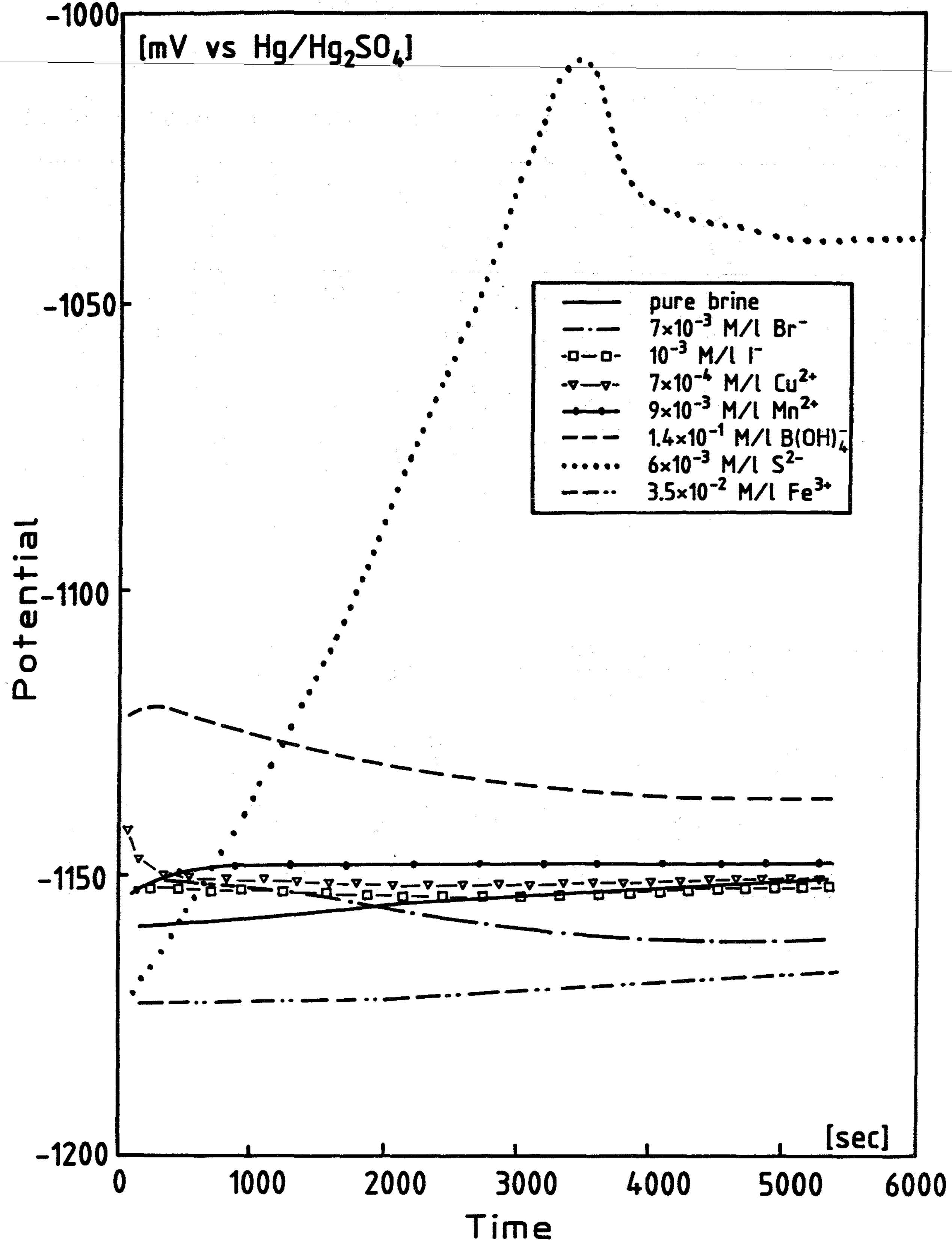

Fig. 1: Free corrosion potential as function of time of the fine-grained steel TStE 355 at 90° C in NaCl-rich brine (pH = 7) with and without additions

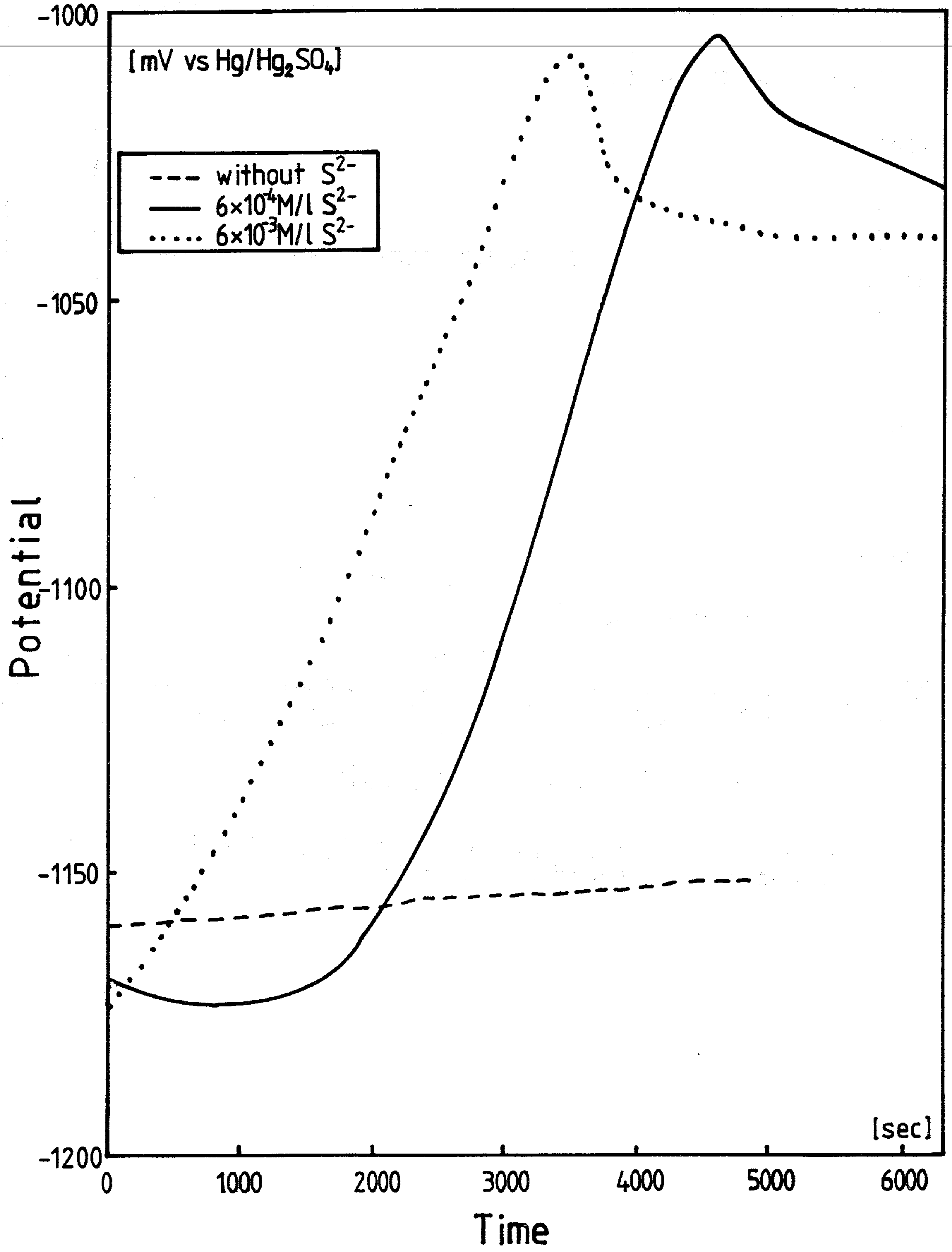

Fig. 2: Free corrosion potential as function of time of the fine-grained steel TStE 355 at 90° C in NaCl-rich brine (pH = 7) with and without sulfides

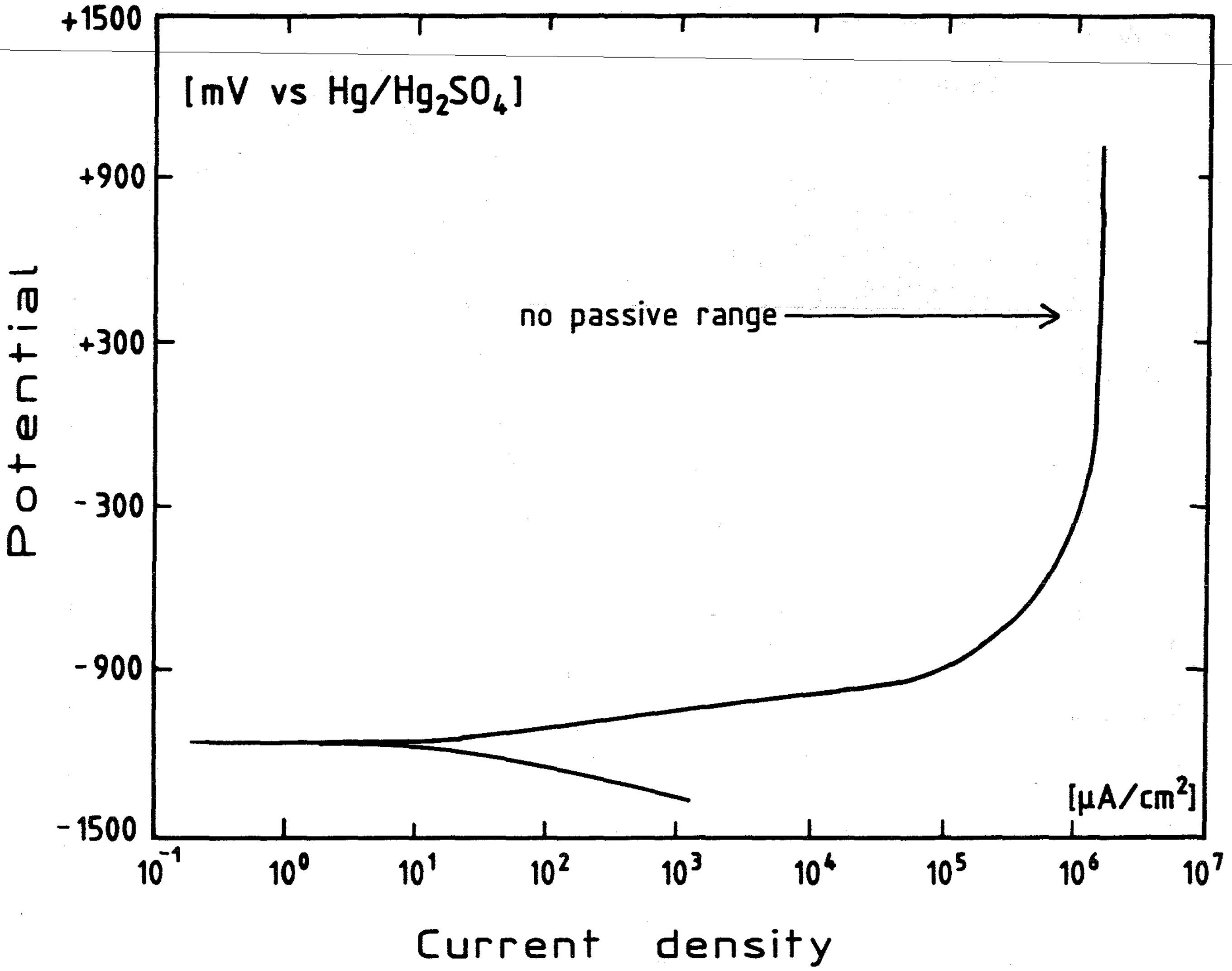

Fig. 3: Potentiodynamic polarization curve of the fine-grained steel TStE 355 in deaerated NaCl-rich brine at 90 °C (pH = 7)

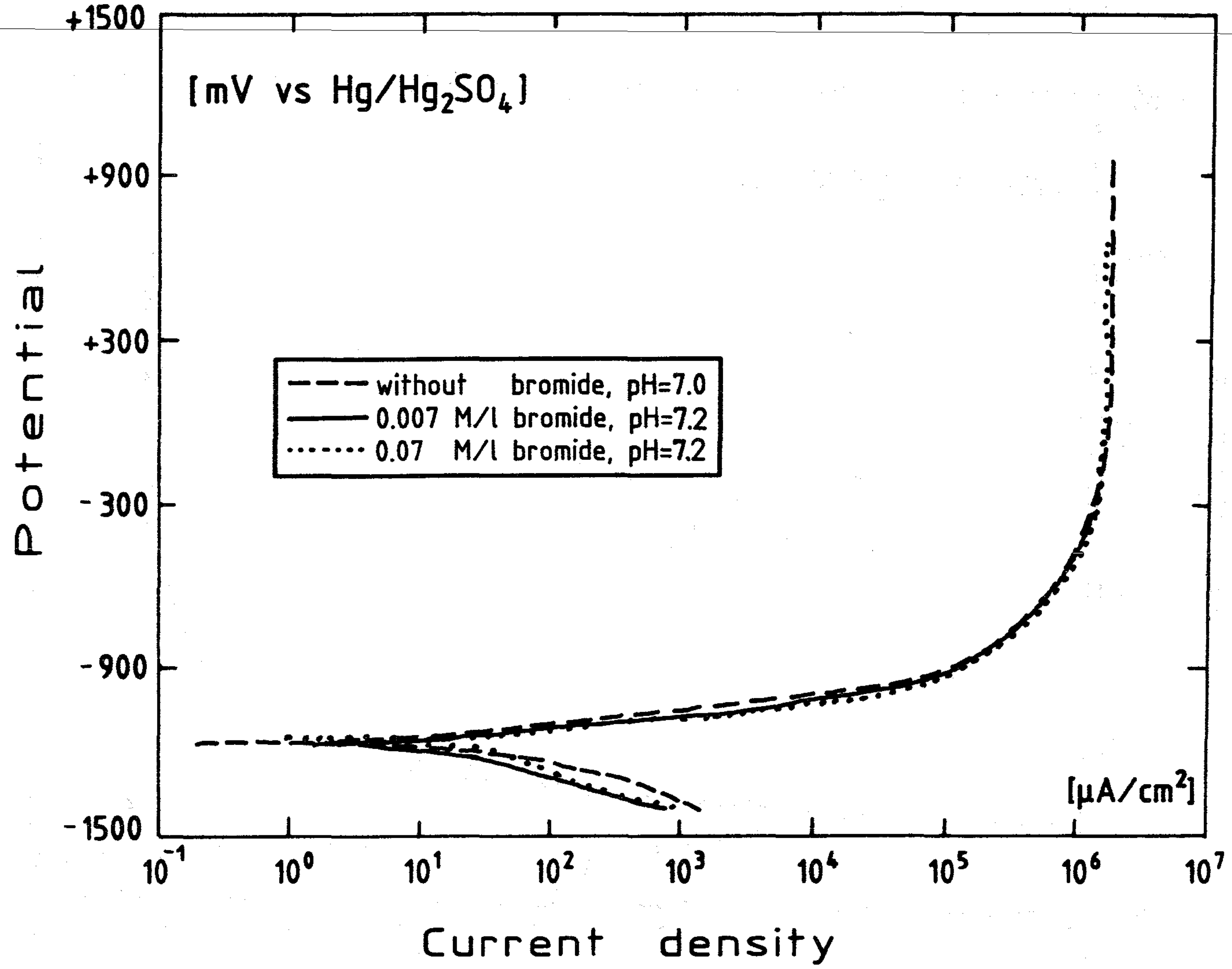

Fig. 4: Potentiodynamic polarization curves of the fine-grained steel TStE 355 at 90 °C in NaCl-rich brine with and without bromides

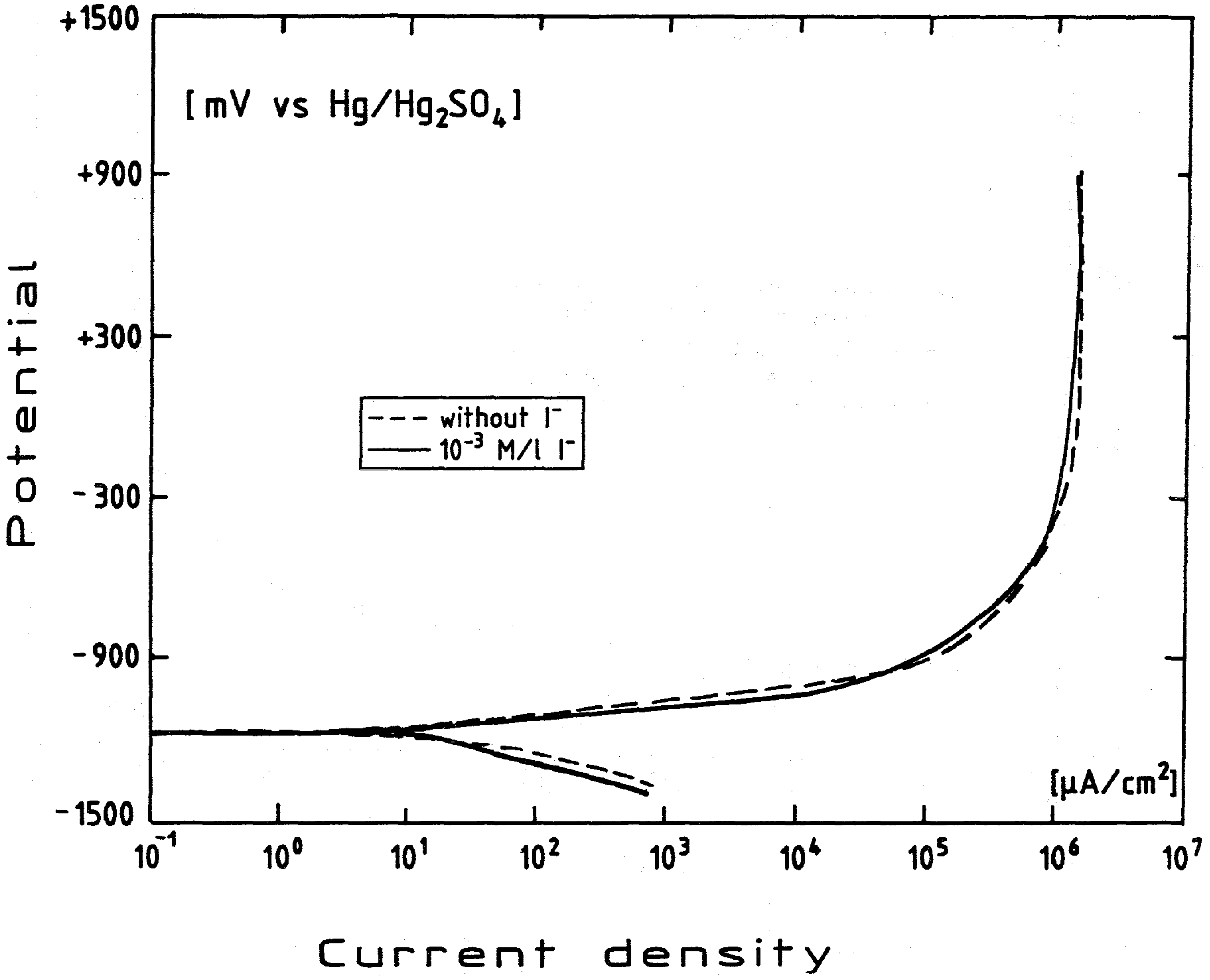

Fig. 5: Potentiodynamic polarization curves of the fine-grained steel TStE 355 at 90 °C in NaCl-rich brine with and without iodides (pH = 7)

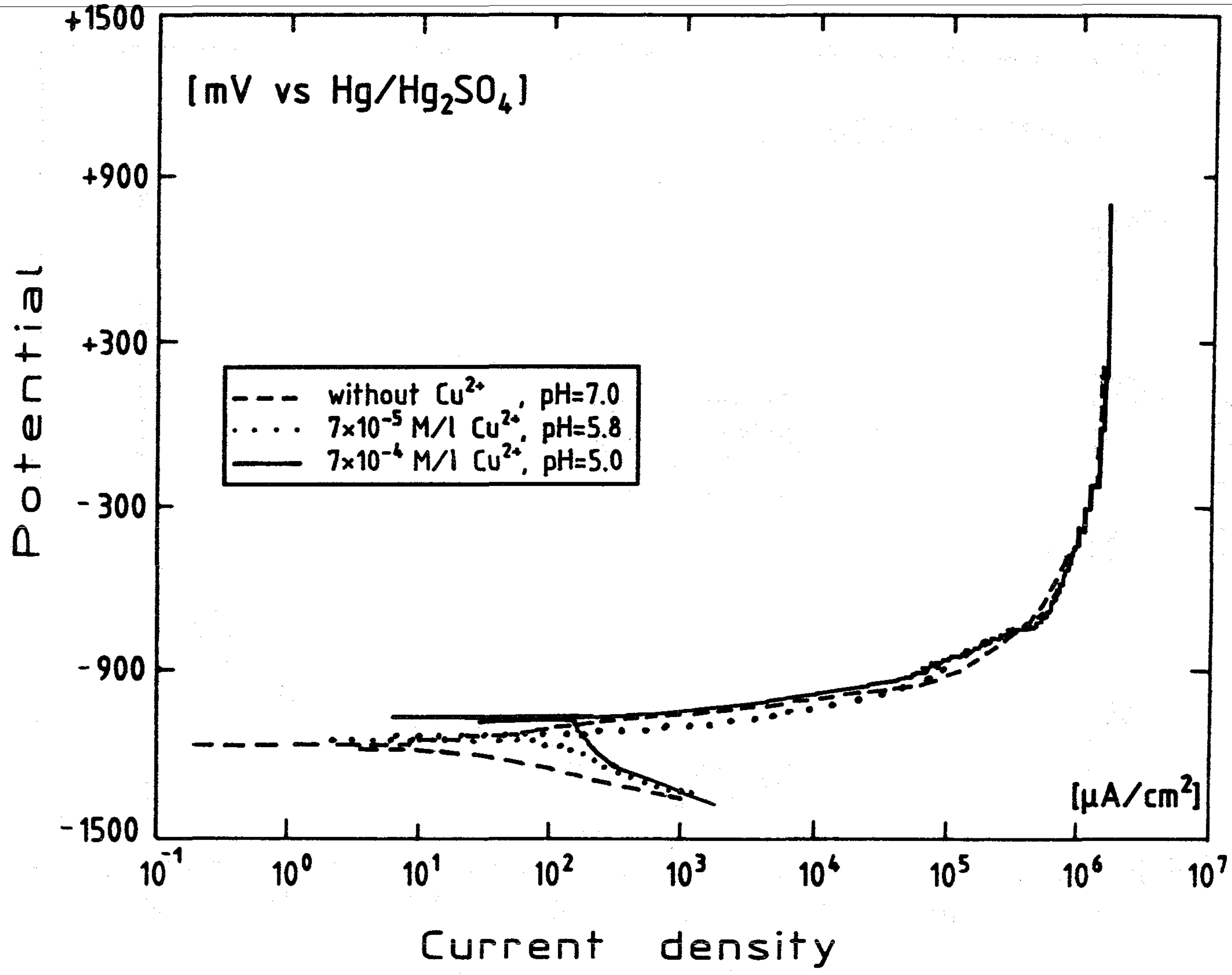

Fig. 6: Potentiodynamic polarization curves of the fine-grained steel TStE 355 at 90 °C in NaCl-rich brine with and without cupric ions and various pH-values

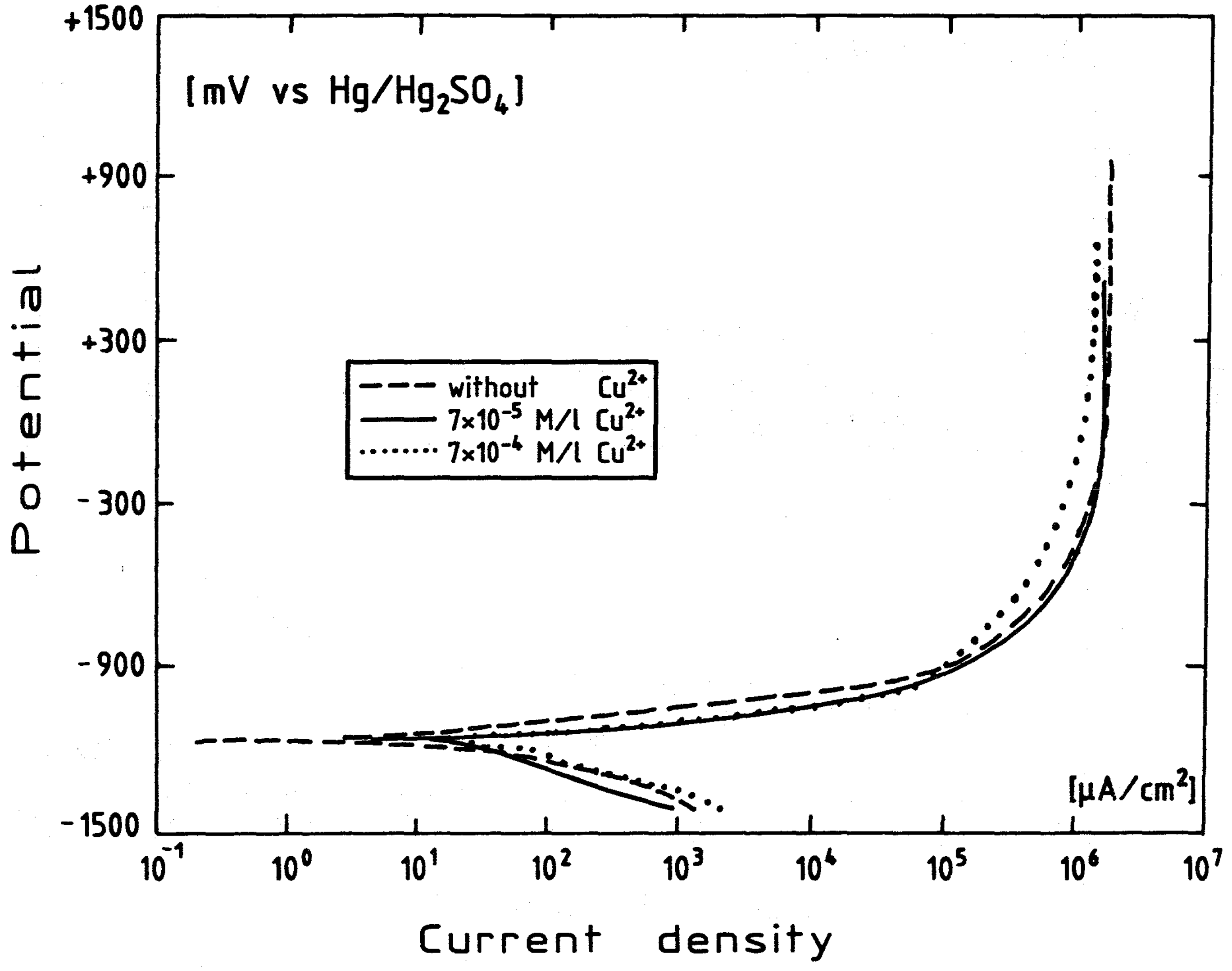

Fig. 7: Potentiodynamic polarization curves of the fine-grained steel TStE 355 at 90 °C in NaCl-rich brine with and without cupric ions (pH = 7)

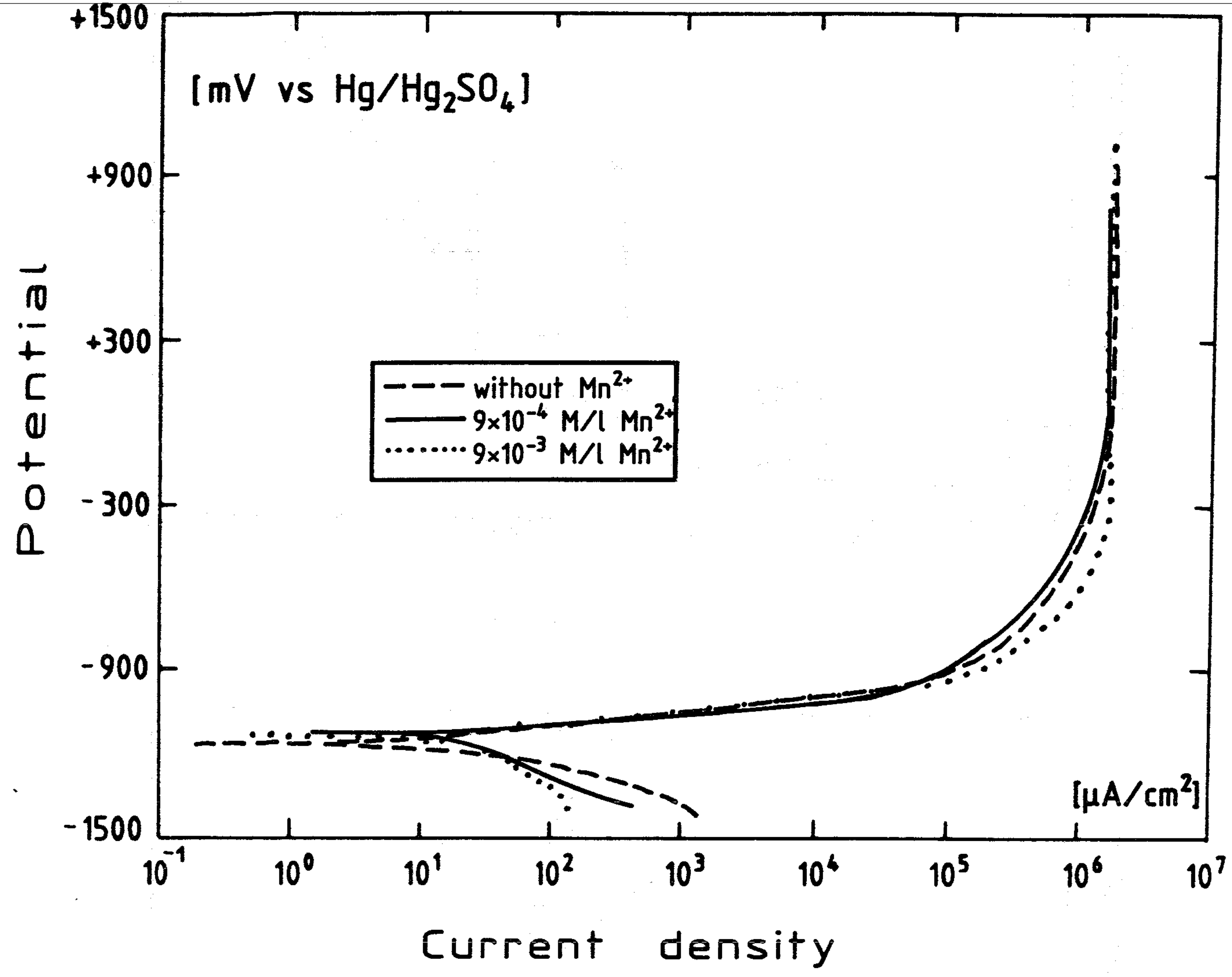

Fig. 8: Potentiodynamic polarization curves of the fine-grained steel TStE 355 at 90 °C in NaCl-rich brine with and without manganese ions (pH = 7)

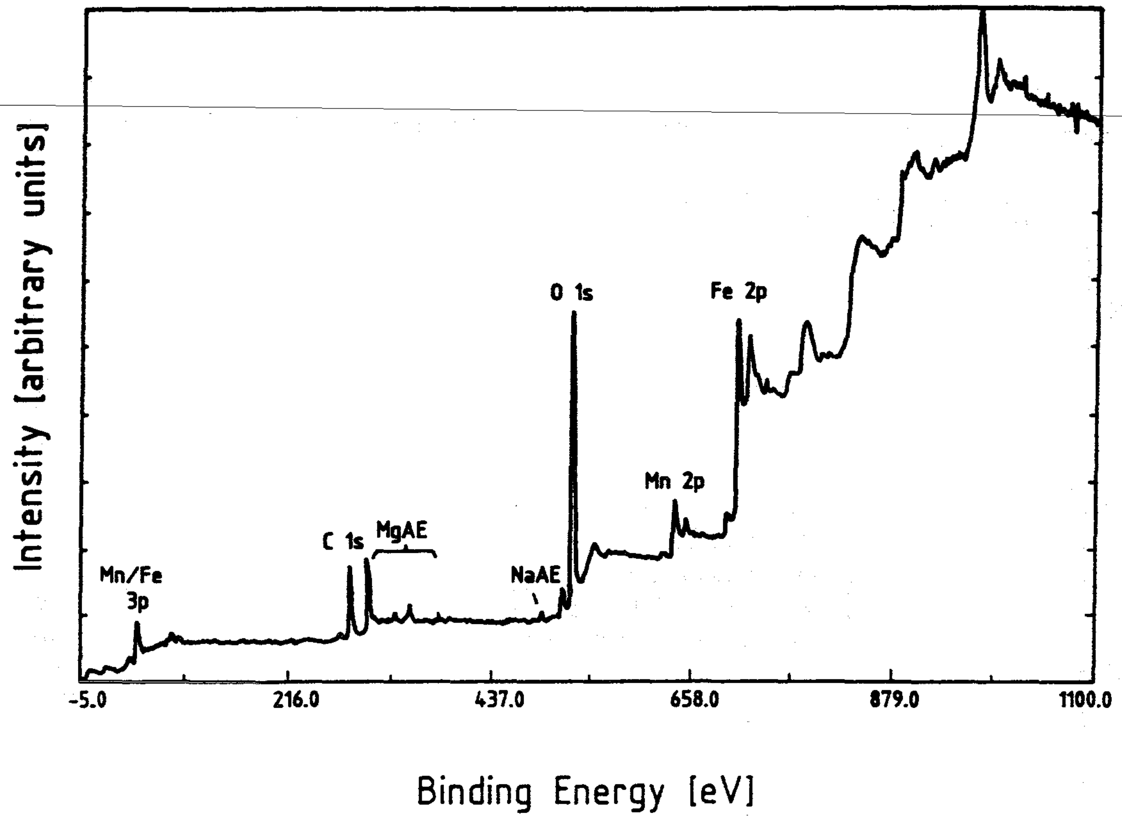

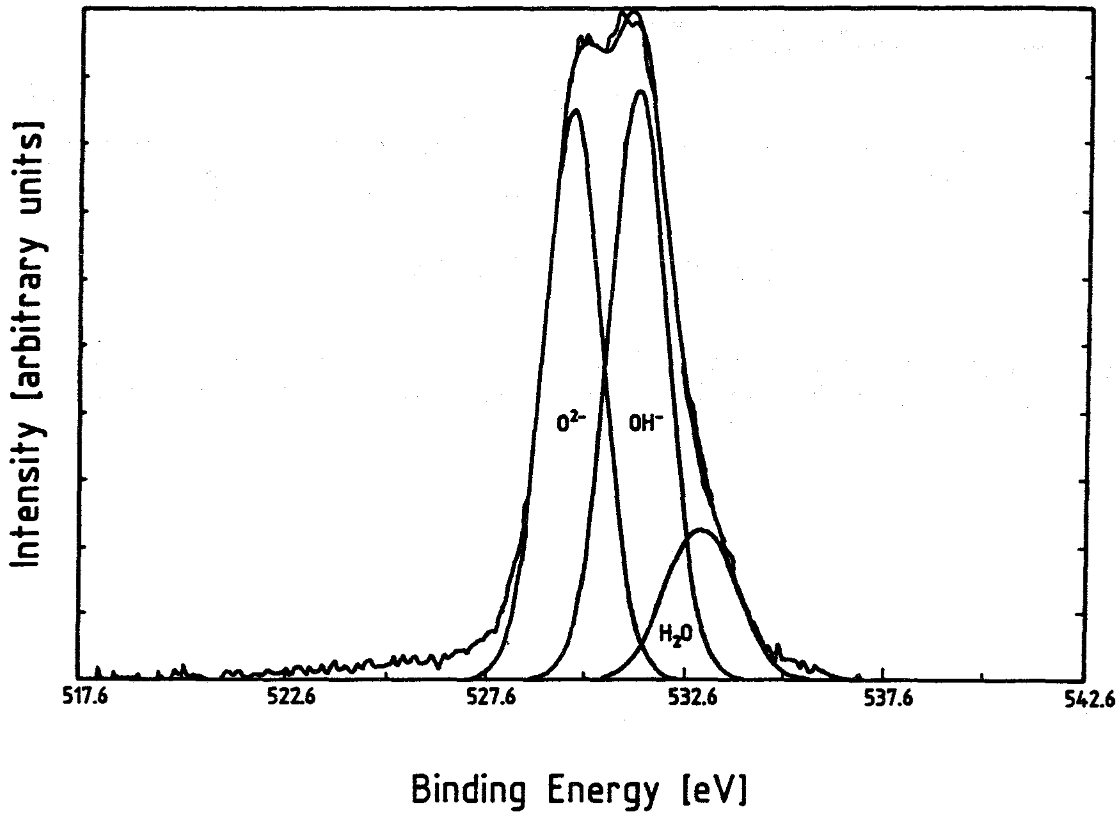

Fig. 9: XPS spectra of corrosion products on specimens of the fine-grained steel TStE 355 maintained at free corrosion potential in NaCl-rich brine + 9 x 10^{-3} M/l Mn^{2+} at 90 °C

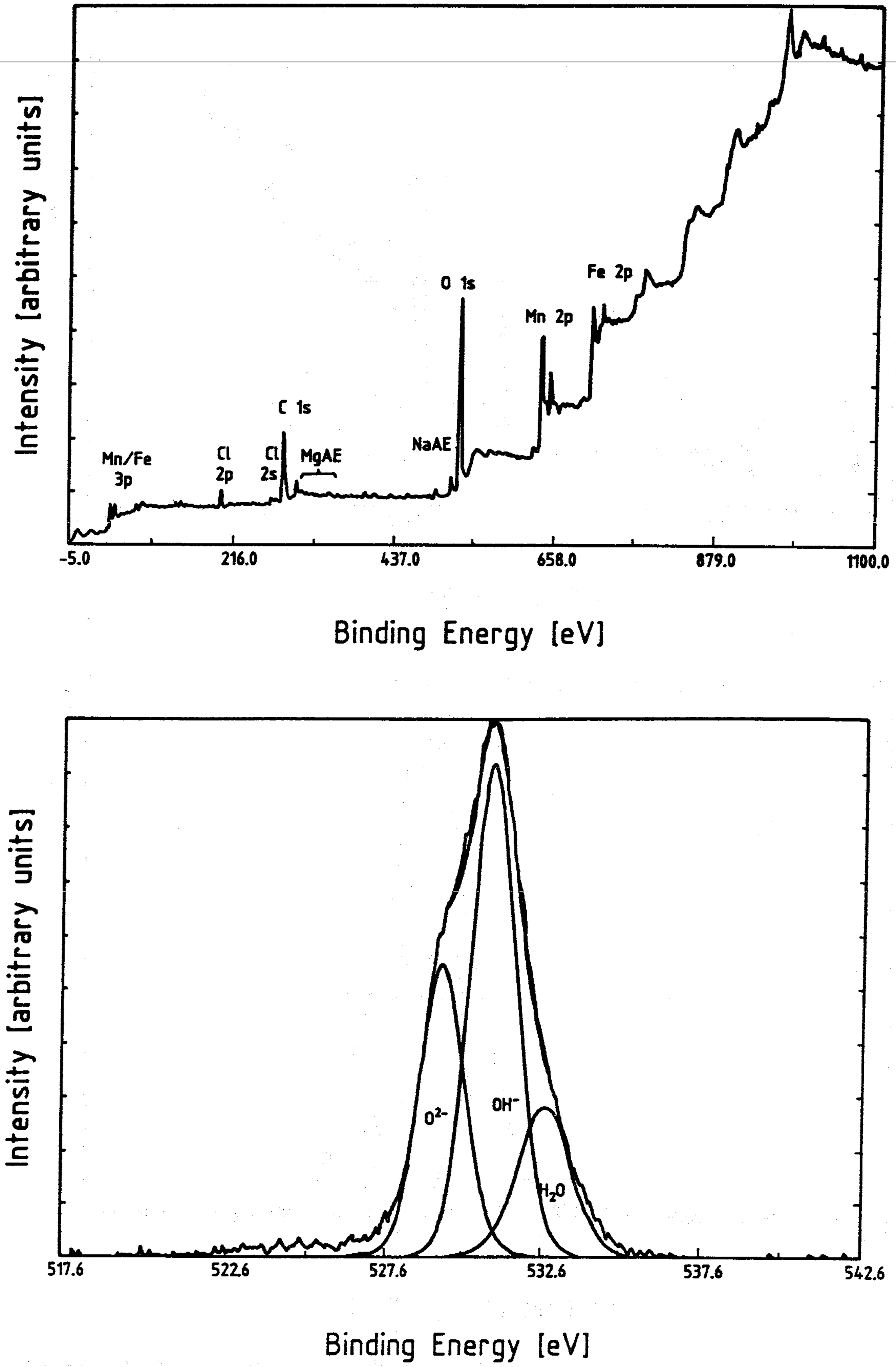

Fig. 10: XPS spectra of corrosion products on specimens of the fine-grained steel TStE 355 following cathodic polarization in NaCl-rich brine + 9 x 10^{-3} M/l Mn^{2+} at 90 °C

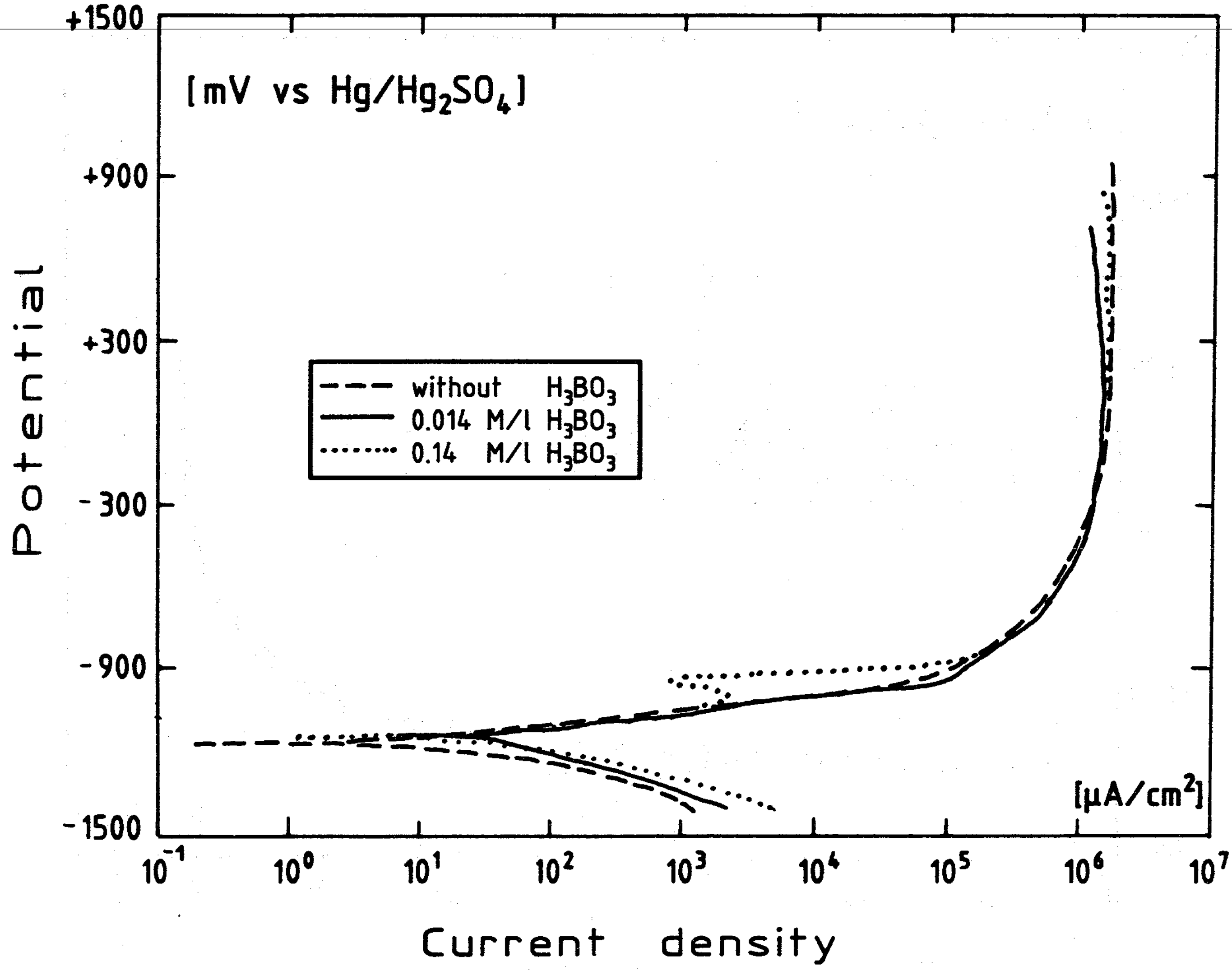

Fig. 13: Potentiodynamic polarization curves of the fine-grained steel TStE 355 at 90 °C in NaCl-rich brine with and without borate ions (pH = 7)

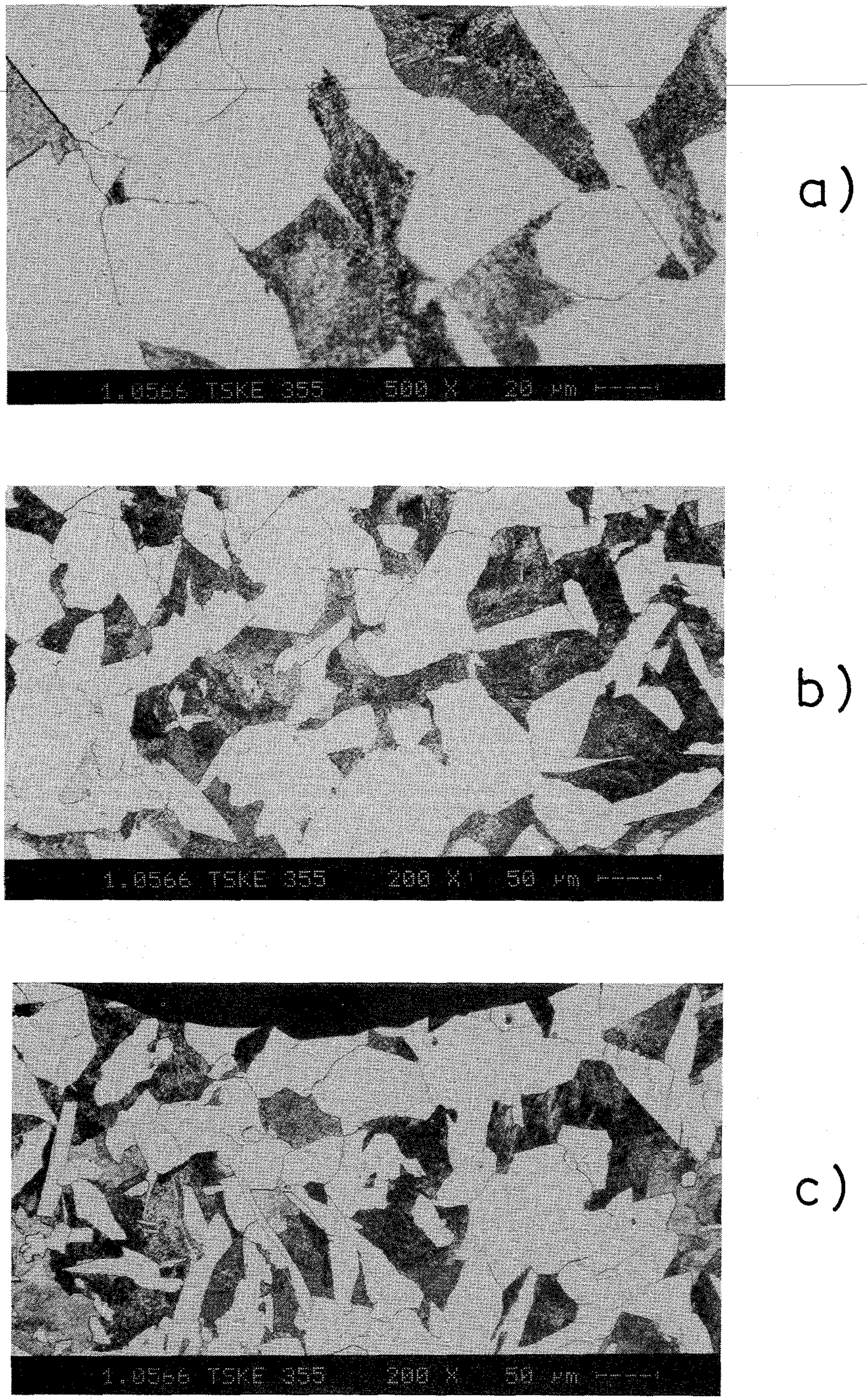

Fig. 14: Optical micrographs of fine-grained steel specimens (TStE 355) following potentiodynamic polarization testing in NaCl-rich brine + 0.14 M/l $B(OH)_4^-$ at 90 °C
a) -910 mV b) -880 mV c) + 500 mV vs R.E.

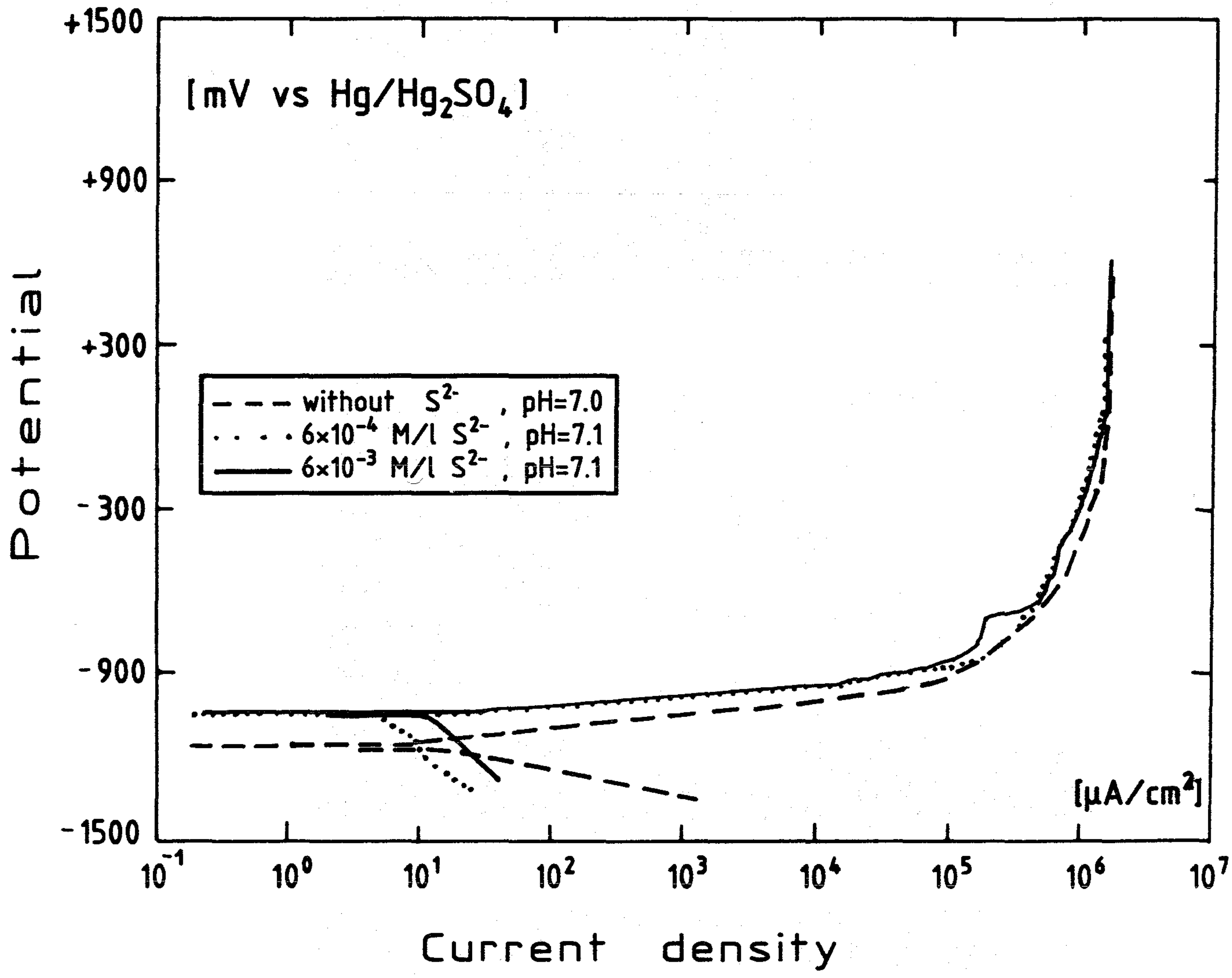

Fig. 15: Potentiodynamic polarization curves of the fine-grained steel TStE 355 at 90 °C in NaCl-rich brine with and without sulfide ions (pH = 7)

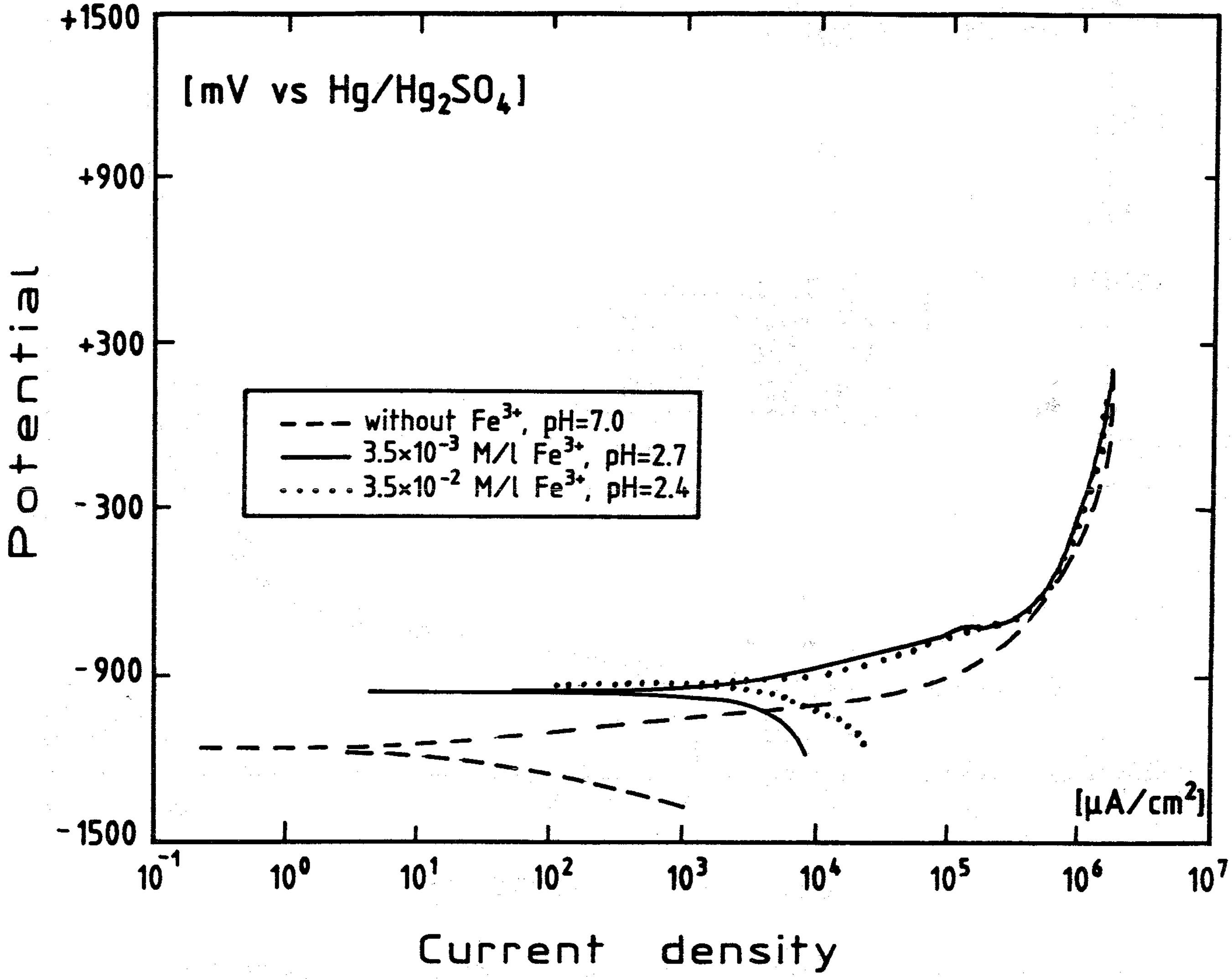

Fig. 16: Potentiodynamic polarization curves of the fine-grained steel TStE 355 at 90 °C in NaCl-rich brine with and without ferric ions and various pH-values

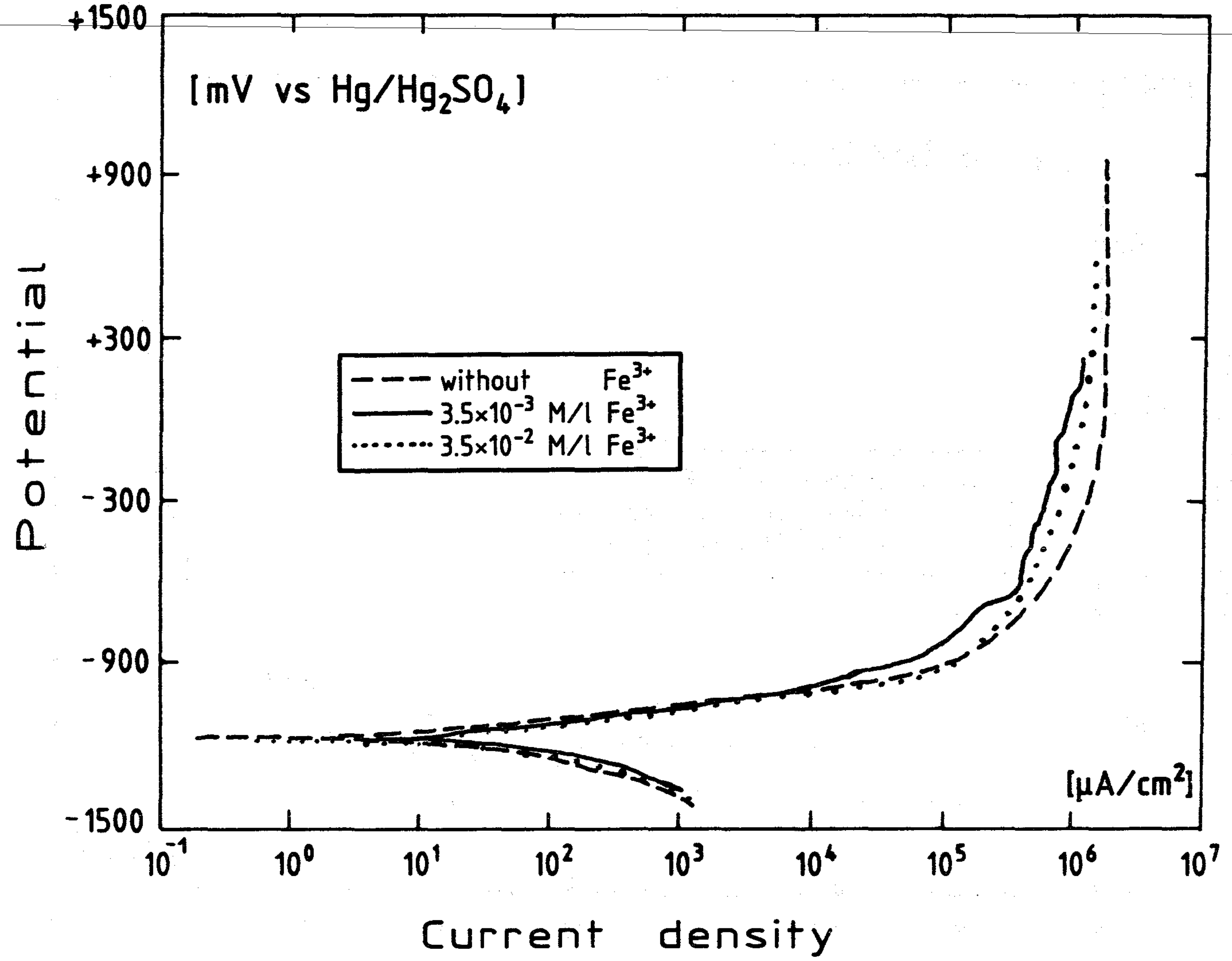

Fig. 17: Potentiodynamic polarization curves of the fine-grained steel TStE 355 at 90 °C in NaCl-rich brine with and without ferric ions (pH = 7)